A Combined Dual-Tree Complex Wavelet (DT-CWT) and Bivariate Shrinkage for Ultrasound Medical Images Despeckling

Romain Mavudila Kongo
LETS Laboratory
Physics Department
Mohamed V University
Rabat, Morocco.

Mohammed Cherkaoui
Faculty of Medicine and pharmacy
Fès, Morocco

Lhousaine Masmoudi
& Najem Hassanain
3rd author'sLETS Laboratory
Physics Department
Mohamed V University
Rabat,Morocco

ABSTRACT

In this paper, an efficient DT-CWT based method for medical ultrasound images despeckling is presented. The ultrasound images are often deteriorated by speckle noise, this noise is a random granular texture that obscures anatomy in ultrasound images and degrades the detectability of low-contrast lesions. Speckle noise occurrence is often undesirable, since it affects the tasks of human interpretation and diagnosis.Different from many other schemes with wavelet transform are used on one side in which the studies have dealt more with the standard DWT case. However, the Discrete Wavelet Transform (DWT) has some disadvantages that undermine its application in image processing.In this study we investigated a performances complex wavelet transform (DT-CWT) combined with Bivariate Shrinkage.The proposed method was tested on a noisy ultrasound medical image, and the restored images show a great effectiveness of DT-CWT method compared to the classical DWT.

Keywords

Medical image denoising, Medical ultrasound , speckle noise, Dual-tree wavelet transform , Complex wavelet , Bivariate shrinkage

1. INTRODUCTION

We Ultrasound echography technique is one of the most widely used in medical analysis and diagnosis domain, since it permits to observe all kinds of soft tissues in a non-invasive way.

The interpretation of ultrasound images remains a difficult task due to the inherent speckle noise in the images which affects the detectability of low contrast lesions.

The speckle noise is usually described than it is created by complex interference of ultrasound echoes and variations in tissues attenuation, propagation and scattering properties make echoes interfere in complex ways [1].

Many techniques have been developed in the goal to restore ultrasound images such as adaptive filters [2] anisotropic diffusion [3] [4][5] and wavelet shrinkage [6] [7].

The last one have become more prevalent in the transform domain despeckling community owing to their excellent spatial localization, frequency spread and multiresolution characteristics, which are similar to theoretical models of the human visual system (HVS) [8].

Many challenges have been made to remove this noise using wavelet transform [9][10]. A comparative study have been reported by Mariana Carmen and al where it has been proved that the discrete wavelet transform gives a much better result than the spatial filtering methods for despeckling ultrasound images[11].

In the wavelet domain, the Discrete Wavelet Transform (DWT) have limits and major disadvantages that undermines its application for some image processing as; lack of shift invariance, poor directional selectivity for diagonal features and others [12].

Being motivated by applications and advantages of wavelet transform domain, considering these previous results in the literature, in the ultrasound images denoising, we focus our approach by working to put the extension in Dual-Tree Wavelet transform (DT-CWT) case, to its best directional selectivity and using steps of pre- and post- processing, providing significant stake in the study of statistical noise[8].

The most promising Dual-Tree wavelet Transform (DT-CWT) proposed by N. Kingsbury, used two classical wavelet trees developed in parallel with filters forming (approximate) Hilbert pairs looking into the benefits such as good directional selectivity in two-dimensions (2D) approximate shift invariance, the orientation of the wavelets and perfect signal reconstruction (PR) have come to resolve all these problems [13].

To restore the ultrasound images in the complex wavelet domain is very easy and provides the spatially varying spectral characteristics required for de-noising in additional the existence of dual tree is the advantage in the study of statistical noise.

In this, an efficient DT-CWT combined with a Bivariate estimator based method for despeckling ultrasound medical images is proposed.

2. SPECKLE NOISE STUDY

The presence of scatters smaller than the wavelength creates the so-called speckle noise. It is a random, deterministic image patterning caused by the interference of the sub-resolution scattered echoes. Its texture does not contain information about the underlying tissue.It mean brightness does in principle reflect the brightness of the tissue.

Speckle has been widely studied in the literature. In this context Pioneering and distinguishing works have been done by Goodman [14].

The first discussion of ultrasound speckle using statistical optics can be found by Burckhardt [15]. A classic paper on the second-order statistics of speckle is by Wagner et al. [14].

A discussion of Rician statistics in tissue characterization was being studied by Insana and al. [2].

Assuming that the statistics of the RF signal are White Gaussian and the scatters are independent.The envelope-detected signal follows a Rice distribution equation:

$$P() = \frac{}{\sigma^2} \exp\left(-\frac{^2+s^2}{2\sigma^2}\right) I_0 \frac{s}{\sigma^2} , \ge 0 \qquad (1),$$

Wherea is the mean scatter spacings is the strength of a specular reflector, σ is the standard deviation of noise and I_0 is the incomplete Bessel function of order zero. The Rician PDF is parameterized by a single parameter k, which is defined as:

$$k = \frac{s}{\sigma} \qquad (2)$$

The Rician distribution reduces to the Rayleigh distribution for the special case $s = 0$, that is, when there are no bright scatters. Then the image consists in purely speckle patterning due to sub-resolution scatters. The Rayleigh distribution is defined in [2] by equation:

$$P() = \frac{}{\sigma^2} \exp\left(-\frac{^2}{2\sigma^2}\right) , \ge 0 \qquad (3)$$

However log-compression changes the characteristics of the signal probability distribution.

In particular, it affects the high intensity tail of the Rayleigh and Rician more than the low intensity part. Strictly the log-compression on Rician document is a Fisher-Tippett distribution is expressed as:

$$P() = \frac{\exp{(-z)^z}}{\beta} \qquad (4)$$

And

$$z = \exp\left(\frac{-u}{\beta}\right) \qquad (5)$$

However, some approximations can be made. If it is considered as Gaussian, Kao et al. [16] demonstrate that speckle noise distribution can be approximated as an additive colored Gaussian PDF. Abd-Elmoniem et al. assume that in a reasonably high number of scatters; that is not too low SNR additive white Gaussian noise is a good approximation. From our experiments, the additive colored Gaussian noise is the most satisfying model.

Many techniques have been proposed to reduce speckle including spatial filtering [3][5][17]18] temporal integration [19] frequency compounding [20] and spatial compounding [21][22].

Generally speckle is modeled as multiplicative noise and its reduction is done by multiplying wavelet coefficients by speckles reduction ratio.

The mathematical expression for a signal observed at point whose coordinates (x, y) in the ultrasound image is as follows:

Assuming that speckle noise to be fully developed and independent of 'f' so we can write:

$$g(x, y) = f(x, y).\mu(x, y) + \varepsilon(x, y) \qquad (6)$$

With $g(x, y)$, $f(x, y)$ and $\mu(x, y)$, where (x, y)$^{-th}$ pixel's ultrasound image andthe corresponding tissue-reflectivity at the speckle noise.

$\varepsilon(x, y)$is an additive noise [23] and can be ignored in practice.

$\mu(x, y)$is a noise independent from the signal. In the following the model used for the ultrasound image is:

$$g(x, y) = f(x, y) * \mu(x, y) \qquad (7)$$

Where g is the observed intensity of the image and f is is the free noise intensity. Within homogenous regions this model offers as good approximation [24][25].

To cover the multiplicative noise an additive one the noise image is log-transformed yielding.

$$G(x, y) = F(x, y) + U(x, y) \qquad (8)$$

WhereG, F and U are the logarthms of g, f and μ respectively. Now it is demonstrated that speckle noise distribution can be approximated as additive Gaussian [16]. In considering the linearity Property in the noise study as with any redundant frame analysis; when a stationary noise even if white is subject to a dual decomposition tree statistical dependencies appear between coefficients [26][27].

After applying the DT-CWT on (8), we obtain:

$$G_\eta(x, y) = F_\eta(x, y) + U_\eta(x, y) \qquad (9),$$

Where, $G_\eta(x,y)$, ,$F_\eta(x,y)$ and $U_\eta(x,y)$, denote (x,y)$^{-th}$ wavelet coefficient at level η of a particular detail subband of the DT-CWT of G,F and U respectively and η (η= 1,2…,J).
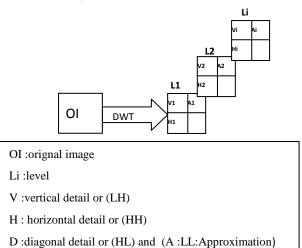
3. WAVELET TRANSFORM APPROACH
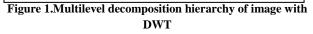
3.1 Discrete Wavelet Transform (DWT)

The implementation of an analysis filterbank for a single level 2D-DWT with the algorithm of Mallat on the decomposition of an image, with two filter banks low pass and high pass respectively .

This structure produces detailed sub-images (HH,HL and LH) corresponding to three different directional-orientation (horizontal, vertical and diagonal) and a lower resolution sub-image (LL) [28].

The filter bank structure can be iterated in a similar manner on (LL) channel to provide multilevel decomposition as illustrated in Fig. 1.

OI :orignal image

Li :level

V :vertical detail or (LH)

H : horizontal detail or (HH)

D :diagonal detail or (HL) and (A :LL:Approximation)

A : approximation

Figure 1.Multilevel decomposition hierarchy of image with DWT

The classical discrete wavelet transform (DWT) provides a means of implementing a multiscale analysis based on a critically sampled filter bank with perfect reconstruction [21]. However questions arise regarding the good qualities or properties of the wavelets and the results obtained using these tools; the standard DWT suffers from the following problems described as below.

-Shift sensitivity: it has been observed that DWT is seriously disadvantaged by the shift sensitivity that arises from down samples in the DWT implementation [12][13].

-Poor directionality: an m-dimension transform (m>1) suffers poor directionality when the transform coefficients reveal only a few feature in the spatial domain.

-Absence of phase information: filtering the image with DWT increases its size and adds phase distortions; human visual system is sensitive to phase distortion [16]. Such DWT implementations cannot provide the local phase information.
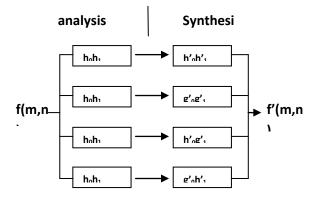
In other applicationsand for certain types of images it is necessary to think of other more complex wavelets which gives a good way because the complex wavelets filters which can be made to suppress negative frequency components. As we shall see the CWT has improved shift-invariance and directional selectivity [29].

3.2 Dual-Tree Complex Wavelet Transform (DT-CWT)

The discrete and complex dual tree wavelet transform (DT-CWT) was introduced by N. Kingsburg around in 1990.

This implementation uses consists in analyzing the signal by two different DWT trees, with filters chosen so that at the end, the signal returns with the approximate decomposition by an analytical wavelet.

The dual-tree structure has an extension of conjugate filtering in 2-D case, this structure is shown in Fig. 2

Imaginary trees

Figure.2. Filterbank structure for DT-DWT

This structure needs four trees for analysis as well as for synthesis. The pairs of conjugate filters are applied to two dimensions (0 and 1), wich can be expressed as:

$$(h_0 + jg_0)(h_1 + jg_1) = (h_0h_1 - g_0g_1) + j(h_0g_1 + g_0h_1)$$
$$(10)$$

The synthesis of filters suitable for this structure was performed by several people.

The wavelet corresponding to the tree's "imaginary part" is very close to the Hilbert transform of the wavelet corresponding to the trees "real part" [30].

For J level decomposition, the corresponding details subbands at leven η are denoted: HLη^{real}, HLη^{im},LHη^{real}, LHη^{im}, HHη^{real} and HHη^{im}, where η = 1,2,….,J.

Because of the existence of two trees, it appears that the second noise coefficients moments from such decomposition can be precisely characterized.

The DT-CWT ensures filtering of the results without distortion and with a good ability for the localization function and the perfect reconstruction (PR) of signal.

In the noise study, as with any redundant frame analysis, when a stationary noise, even if white, is subject to a dual decomposition tree, statistical dependencies appears in coefficients [12][26][27]because of the existence of two trees.It appears that the second noise coefficients moments from such decomposition can be precisely characterized.

We observe a decorrelation between primal and dual coefficients located at the same spatial position and an interscale correlation which allows us to choose between several estimators taking this phenomenon into account.

If we consider an image degraded by a Gaussian n white centered additive Gaussian noise with a spectral density; the decomposition coefficients are also affected by that same noise as part of the linearity property.

The noise spectral density can be known or not, we can use a robust estimator calculated from the coefficients of the higher frequency bands [29][31][32].

With this advantage we can choose an appropriate estimator for denoising and by the case of DT-DWT we will estimate the spectral density in each tree.

4. THE BIVARIATE MAP ESTIMATOR

Implemented by LeventSendur and Ivan W. Seselesnick [33] gives a performance for image denoisingexploiting the statistical dependence between wavelet coefficients and their 'parents'.

In considering these image as corrupted by additive independent white Gaussian noise with variance σ^2_b

In the multiresolution domain, if we use the orthogonal wavelet transform, the de-noising problem can be formulated as follows:

$$y = w + b \qquad (11)$$

$y$being the noise coefficient, w, the original coefficient, and b, corresponding to the Gaussian independent noise. Our goal is to estimate $w$from y. To do this we will use an MPE (Maximum Posterior Estimator) filter [34].

Let $w_{2\eta}$ represent the'' parent'' of $w_{1\eta}$; where $w_{2\eta}$ is the wavelet coefficient at the same position as the ηth wavelet coefficient $w_{1\eta}$, but at the next coarser scale .

In wavelet domain the problem have been formulated as *follow:*

$$y_{1\eta} = w_{1\eta} + b_{1\eta} \text{and} y_{2\eta} = w_{2\eta} + b_{2\eta} \qquad (12),$$

Where

$y_\eta = (y_{1\eta}, y_{2\eta})$: noisy coefficient (child and parent)

$w_\eta = (w_{1\eta}, w_{2\eta})$: original coefficients

$b_\eta = (b_{1\eta}, b_{2\eta})$: Gaussian independent noise .

If the y_1 coefficient is the considered an detail and y_2 is considered its "parent" (the detail coefficient located in the same geometric position, but calculated in the next iteration.

Each sub-band "parent" coefficient will be over-sampled for the same number of elements than that of the corresponding "children" coefficients shown in Fig3.
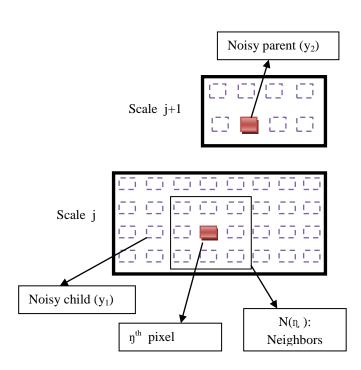

Figure3.Dependency across scales of wavelet coefficients (neighborhood N(ɳ) illustration)

The standard MAP estimator for ω given the corrupted observation y is:

$$\widehat{w}(y) = \text{argmax}_w \left[(\ln(P_{b_\eta}(y_\eta - w_\eta) P_{w_\eta}(w_\eta)) \right] \tag{13}$$

In considering than image as corrupted by additive white Gaussian noise with zero mean we can write:

$$P_{b_\eta}(b_\eta) = \frac{1}{2\pi\sigma_b^2} e^{\frac{b_{1\eta}^2 + b_{2\eta}^2}{2\sigma_b^2}} \tag{14}$$

Using the notation as:

$$f(w_\eta) - \ln(P_{w_\eta}(w_\eta)) \tag{15},$$

Proposed in [34] the model for useful image in wavelet transform as:

$$P_{w_\eta}(w_\eta) = \frac{3}{2\pi\sigma^2} e^{-\frac{\sqrt{3}}{\sigma}\sqrt{(w_{1\eta}^2) + (w_{2\eta}^2)}} \tag{16}$$

Where, w_η represents the set of coefficients on the ηth of wavelet transform of useful image calculated to ɳth iteration and $w_{2\eta}$ is the set of coefficients of the useful image calculated to the next iteration.

The equation of the MAP filter defined in (13) and (14) takes the form defined in:

$$\widehat{w_\eta}(y_\eta) = argmax_{w_\eta}\{-\frac{(y_{1\eta}-w_{1\eta})^2 - (y_{2\eta}-w_{2\eta})^2}{2\sigma_\eta^2} + f(w_\eta)\} \tag{17}$$

This form is equivalent to the equation system:

$$\frac{(y_{1\eta}-w_{1\eta})^2}{\sigma_b^2} + \frac{\alpha f(w_\eta)}{2w_\eta} = 0 \tag{18}$$

$$\frac{(y_{2\eta} - w_{2\eta})^2}{\sigma_b^2} + \frac{\alpha f(w_\eta)}{2w_\eta} = 0$$

i.e :

$$\frac{(y_{1\eta}-w_{1\eta})^2}{\sigma_b^2} + f_1(w_\eta) = 0 \tag{19}$$

$$\frac{(y_{2\eta} - w_{2\eta})^2}{\sigma_b^2} + f_2(w_\eta) = \upsilon$$

Considering the definition of the function f, we can write :

$$f(w_\eta) = \ln P_{w_\eta}(w_\eta) \tag{20}$$

Taking into account the density of probability expressed in (14), the system of equation in the form as:

$$\frac{(w_{1\eta}-y_{1\eta})^2}{\sigma_b^2} - \frac{\sqrt{3}}{\sigma}\frac{\widehat{w_{1\eta}}}{\sqrt{w_{1\eta}^2+w_{2\eta}^2}} = 0 \tag{21}$$

$$\frac{(w_{2\eta} - y_{2\eta})^2}{\sigma_b^2} - \frac{\sqrt{3}}{\sigma}\frac{\widehat{w_{2\eta}}}{\sqrt{w_{1\eta}^2 + w_{2\eta}^2}} = 0$$

The nth solution of the last equations system is as follows:

$$\widehat{w_{1\eta}} = \frac{\left[\sqrt{x_1^2+y_2^2} - \frac{\sqrt{3}\sigma_\eta^2}{\sigma}\right]_+}{\sqrt{x_1^2+y_2^2}} \cdot y_{1\eta} \tag{22}$$

Which can be interpreted as a bivariate shrinkage function. Here (g)+ is defined as:

$$(g)_+ = \{^{1, \ si \ g<0}_{0, \ otherwise} \tag{23}$$

The marginal variance $\sigma^2$is also dependent on the coefficient index ɳ and sigma for ɳth coefficient will be estimated using neighboring coefficient the region N(ɳ); where N(ɳ) is defined as all coefficients within a square shaped window that in centered at the ɳth coefficient .Fig3 [33]..

The noise variance σ^2_b is estimated from the robust median estimator as follow:

$$\hat{\sigma}_b^2 = \frac{median(|y_i|)}{0.6745} y_i \in sous - band \ HH \tag{24}$$

From this observation model, one gets;

$$\sigma^2 = \sigma_\eta^2 - \sigma_b^2 \tag{25},$$

where$\sigma_\eta^2$is the marginal variance of noisy observations y_1 and y_2.Since y_1 and y_2 are modeled as zero mean,σ_η^2can be found empirically by:

$$\hat{\sigma}_\eta^2 = \frac{1}{M}\sum_{y_i \in N(\eta)} y_i^2 \tag{26}$$

'M' is the size of the neighborhood N(ɳ), than … can be estimated as :

$$\hat{\sigma} = \sqrt{(\hat{\sigma}_\eta^2 - \hat{\sigma}_b^2)_+} \tag{27}$$

4. PROPOSED EXPERIMENTAL METHOD

Consider that the speckle is a multiplicative and with the appropriate estimator (Bivariate shrinkage) method which exploits the inter-scale dependencies relations between the

coefficients and their parents; we can to restore the image with best quality [34].

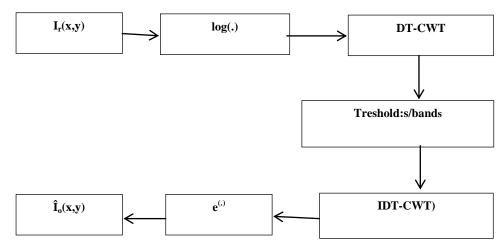The key idea of wavelet shrinkage is that the wavelet representation can separate the signal from the noise.

Fig 4: Diagram of despeckling proposed method.

The despeckling diagram involves the following steps shown in diagram Fig. 4:

(1)Transform the multiplicative noise into an additive, one by taking the logarithm of noised image

(2)Compute the DT-CWT(dual-tree complex wavelet) of the log-transformed image,

(3)Compute the threshold value for each pixel for Visu shrink or applying Bivariate MAP estimator, in all sub band details wavelet coefficients.

(4)We compute the IDT-CWT(inverse dual-tree complex wavelet) and take exponent for obtained the de-noised image

In the case of the classical DWT, we use the estimator on the coefficients obtained.

For DTT, as mentioned above, we used two coefficients sets obtained from the primal and dual trees and treated separately, as if we had two independent wavelet compositions, which brings us back to the application of two estimators, one on each coefficient set.

The logarithm is applied at the image for to transform a multiplicative noise an additive noise before computing it with DT-CWT .

After computing the details wavelet coefficients, will be threshold with appropriates filters chosen, we compute the IDT-CWT this data, finally we obtain the de-noised estimate image $\hat{\imath}_0 (x,y)$ after inverse logarithm.

The performance of the proposed approach is measured in one side by the quantitative measures namely MSE (mean square Error) and PSNR (peak Signal to Noise ration) between host and restored images are determined as :

$$MSE = \frac{1}{MN}\sum_{i=1}^{M}\sum_{j=1}^{N}(X(i,j) - Y(i,j))^2 \quad (14)$$

And,

PSNR (dB) = 10 log10 (2552 /MSE)   (15)

On the other hand, to meet the expectations of clinicians, a test has been increased to physician echograph address, on the quality of images; this test methodology is as follows:

Considering the ultrasound images were anonymized first-time summers and echographs were asked the question, whether the image presented to them is acceptable to the diagnosis and answer, yes or no.

Secondly, restored image compared to the image host for each case placed side by side, this time the original is revealed, the observer will quantify on a scale of 1-9 shown:

1: Inacceptable for diagnosis; 9: No visible difference; 7: No loss of diagnostic information; 5: In the limit the loss of information, discrete anomalies can be omitted; 3: Important diagnostic information can be omitted, degradation affects the interpretation and 1: Unsatisfactory for diagnosis.

In the other hand, to meet the expectations of clinicians, a test

5. RESULTS AND DISCUSSION

Here we present the results, the method described were applied on a two ultrasound images

Fig.5. shows a clean ultrasound imageat leftthis corrupted version atrightand a real medical noisy ultrasound image atmiddle.

Figure. 5. Tree ultrasound noised images (a $_0$.:clean ultrasound image left,b.his noisy image and a. ultrasound noisy image)

The first set of image is obtained by corrupting a clean ultrasound medical image pixels with noising having various standard deviation (ao,b)and the second speckled image is a ultrasound medical image obtained from (www.ee.nmt.ed).A performance of this approach is compared using forward wavelet transform combined withVisu-Shrinkage and Bivariate Shrinkage for each case.

In considering the two cases of despeckling,it is clear from the performance of tables and figures that despeckling capability of CWT(namely DT-CWT) is superior than standard DWT.

In both cases, Visu Shrinkage filtering [36] performs poorer whereas Bivariate Shrinkage performs better.

For each case the performance results for noise conditions as follows:

The first results exhibits better contrast in those areas, are the results obtained with Bivariate shrinkage Fig.6 for each ultrasound medical images.

The result in each figure are presented in the order follow as: DWT at left, real DWT in middle and CWT at right.
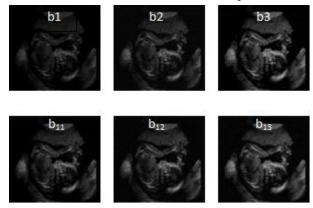

Figure. 6.Shows despeckled medical images with Bivariate Shrinkage (above) and Visu Shrinkage (below); b₁and b₁₁ shows a poor contrast, in general the speckle is efficiently reduced and structures are enhanced with almost no loss or noticeable artifact in other images.

The results of these experiments are confirmed it, in Table I**.** Fig.6.a1and b1   shows a poor contrast, in general the speckle is efficiently reduced and structures are enhanced with almost no loss or noticeable artifact in other images of Fig.6. The results of these experiments are confirmed it, in Table 1.

For the   noisevarianceestimated in order 0.04 in the real speckled medical image, the PSNR values are shown in Table 1, it can be observed that a combined DT-CWT and Bivariate shrinkage gives better results**.**

TABLE.1.**PSNRs VALUES BETWEEN REAL SPECLED IMAGE(..0.04) AND IMAGES DESPLECKING WITH BIVARIATE SHRINKAGE AND VISUSHRINKAGE**.

Real medical ultrasound imge	BIVARIATE SHRINKAGE(,PSNR en dB)	VSUSRHINKAGE (PSRRen dB)
DWT	27.92	26.96
Real DWT	29.145	28.08
CWT	**30.837**	**30.01**

Fig.7, illustrates that, compared to other decompositions, the DT-CWT in CWT version leads to better quality results with fewer artifacts. It can also be seen ,it preserves thin lines or diffuse with DWT. By observed the PSNR values in Table 2,

we can confirm the superiority of DT-CWT combined with Bivariate Shrinkage than with Visu Shrinkage.

TABLE.2.PSNRs VALUES BETWEEN NOISED IMAGES HAVING VARIOUS STANDARD DEVIATIONS AND IMAGES DESPLECKING WITH VISU SHRINKAG (above) AND BIVARIATE

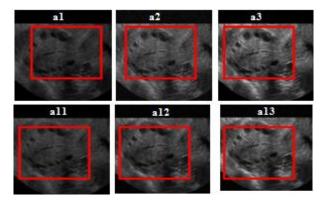| Noise Variance	0.02	0.03	0.04
DWT	27.85	24.19	23.89
Real DWT	30.75	29.13	28.02
CWT	**31.21**	**30.51**	**29.02**
CWT	**32.29**	**31.61**	**30.03**
Real DWT	30.60	30.01	26.10
DWT	28.15	26.48	25.70

SHRINKAGE (below).

Figure7.shows the despeckled (corrupted) images with Bivariate Shrinkage (ebove) and Visu Shrinkage (below), it's shown a strong contrast ,with DWT, admissible results with RDWT and better for CWT.

In comparison the despeckling or thresholding methods chosen, it may be noted that the poorer performances are obtained with DWT, which remains well below the Bivariate Shrinkage.The results are shown in quite similar as shown in Fig 8& 9. Where the graph shows this superiority.
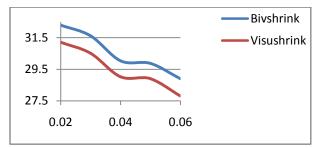

Fig8. Comparison Chart of PSNR of DT-CWT applying with Bivariate estimator and VisuShrinkage in the set of corrupted medical ultrasound images

In additional for the test result it shows the following observation for each case**:**

In case where original image is revealed, we have the following result:

Each ultrasound medical images were considered acceptable for diagnosis by all observers for all DT-CWT in CWT and real version with each estimator.

In case where original image is revealed, we have the following result:

Real ultrasound spekled image: 75% of observers found no significant loss of diagnostic information by real DWT and CWT.

An observer too suggested that the images DWT are degraded to be retable with Visu Shrinkage.

Corrupted image: an observer has seen a restored image with DWT recorded 5. Overall the test result supports the previous confirmations in all case.

All observers agreed on the absence of significant loss of diagnostic information for real DWT and CWT images with the Bivariate estimator Figures Shown.
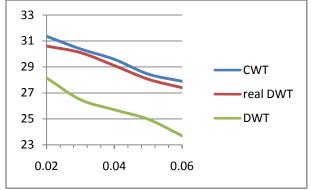

Fig9. **Comparison Chart of PSNR of forward wavelet transforms applying in the set of corrupted medical ultrasound images with Bivariate estimator.**

6.CONCLUSION

We developed and implemented a technique to combine DT-CWT domain and Bivariate shrinkage from different ultransoud medical images to reduce noise and restored the image degraded by this speckle. the presented combined techniques may permit improving the performance of despeckling algorithm.

CWT, which showed to be best in image despeckled did not show the same degree of improvement as in ultrasound medical images for the combined with VisuShrinkage application he experimental results show that the proposed method considerably improves the image quality without generating any noticeable artifact, and provides an additional better performance compared the existing algorithm in the literature.

Noise within ultrasound images was reduced in some techniques, although this showed to have less relevance for clinical practice than border delineation. The analysis shows that there are regions were noise was completely eliminated without affecting either edges or texture. Since all sub-images of details of a given DWT have zero mean value the denoising method proposed the approximation sub-images are not filtered.

The Bivariate Shrinkage filter does not change the mean of processed images; the results obtained with the proposed approach have been made availed to clinicians and proved diagnoses.

7.ACKNOWLEDGEMENTS

6. REFERENCES

[1] J.W. Goodman. 1985. Statiscal optics. Wiley-interscience, New york.

[2] Insana, M. F., Wagner, R. F., Garra, B. S., Brown, D. G., and Shawker, T. H. (1986). Analysis of ultrasound image texture via generalized rician statistics. Optical Engineering, 25(6):743-748

[3] Krissian, K., Vosburgh, K., Kikinis, R., and Westin, C.-F. (2004). Anisotropic diffusion of ultrasound constrained by speckle noise model. Technical Report 0004, Department of Radiology, Brigham and Women's Hospital, Harvard Medical School, Laboratory of Mathematics in Imaging. ISSN.

[4] Montagnat, J., Sermesant, M., Delingette, H., Malandain, G., and Ayache, N. (2003). Anisotropic filtering for model-based segmentation of 4d cylindrical echocardiographic images. Pattern Recognition Letters, 24(4-5):815-828.

[5] Duan, Q., Angelini, E. D., and Laine, A. (2004). Assessment of fast anisotropic diffusion and scan conversion of real-time three-dimensional spherical ultrasound data for visual quality and spatial accuracy. In SPIE International Symposium on Medical Imaging, volume 5370, pages 526{537.

[6] Gupta, S., Chauhan, R. C., and Sexana, S. C. (2001). Wavelet-based statistical approach for speckle reduction in medical ultrasound images. Med. Biol. Eng. Comput., 42:189{192.

[7] Achim, A., Bezerianos, A., and Tsakalides, P. (2001). Novel bayesianmultiscale method for speckle removal in medical ultrasound images. IEEE Transactions on Medical Imaging, 20(8):772{783.

[8] N.G Kinsbury 1998. The dual-tree complex wavelet transform: a new technique for shift invariance and directiona filters. In Proceedings of IEEE Digital Signal Processing Workshop.

[9] A.Pizurica, W.Philips and al 2003 . A versatile wavelet domain noise filtration technique for medical imaging . IEEE Trans. Medical Imaging, vol.22, n° 3, pp. 323-331,

[10] M.Unser and A. Aldroubi 1996. A review of wavelets in biomedical application',proc. Of the IEEE,vol.n°4,pp.626-634.

[11] [11] Mariana Carmen Nicole, LuminitaMoraru and lauraonose 2010 . Comparative Approach for speckle Reduction in Medical ultrasound Images. Vol.ROMANIAJ.BIOPHYS.,Vo. 20,1. P.13-21, BUCHAREST.

[12] N.G Kinsbury2000. A dual-tree complex wavelet transform with improved orthogonality and symmetry proprieties. In Proceedings of the EEE ,Int.Conf. on Image Proc.(ICIP).

[13] N.G Kinsbury 1999. Image processing with complex wavelets. Phil.Trans. Royal Society London.

[14] Goodman, J. W. (1968). Introduction to Fourier Optics. McGraw-Hill, San Francisco.

[15] Burckhardt, C. B. (1978). Speckle in ultrasound b-mode scans. IEEE Transactions on Sonics and ltrasonics, 25(1):1-6.

[16] Kao, C., Pan, X., Hiller, E., and Chen, C. (1998). A bayesian approach for edge detection in medical ultrasound images. IEEE Transactions on Nuclear Science, 45(6):3089{3096

[17] Wagner, R., Smith, S. W., Sandrik, J. M., and Lopez, H. (1983). Statistics of speckle in ultrasound b-scans. IEEE Transactions on Sonics and Ultrasonics, 30(3):156-163

[18] Dutt, V. and Greenleaf, J. (1996). Adaptive speckle reduction _lter for logcompressed b-scan images. IEEE Transactions on Medical Imaging, 15(6):802-813.

[19] Kaplan, D. and Ma, Q. (1994). On the statistical characteristics of the log compressed rayleigh signals: Theorical formulation and experimental results. J. Acoust. Soc. Amer., 95:1396 - 1400.

[20] Evans, A. and Nixon, M. S. (1993). Temporal methods for ultrasound speckle reduction. In IEE Seminar on Texture analysis in radar and sonar, volume 1, pages 1-6.

[21] Cincotti, G., Loi, G., and Pappalardo, M. (2001). Frequency decomposition and compounding of ultrasound medical images with wavelet packets. IEEE Transactions on Medical Imaging, 20(8):764-771.

[22] Trahey, G. E., Smith, S. W., and von Ramm, . T. (1986). Speckle reduction in medical ultrasound via spatial compounding. In Proc. 14th SPIE on Medical Applications, pages 626-637.

[23] AlinAchim, P. Tsakalides, and A. Bezarianos 2001. NovelBayesian multiscale method for speckle removal in medical ul-trasound images. IEEE Trans. on Medical Imaging , vol. 20pp. 772–783.

[24] [Bouc.'01] Samuel Foucher, Gozé Bertin Bénié, Jean-Marc Boucher. January 2001. Multiscale MAP Filtering of SAR images. IEEE Transactions on Image Processing, vol. 10, no.1, , 49-60.

[25] Ali SAMIR ,(2006).Speckle Reduction of ultrasound imaging using wavelet analysis. IMIBE.

[26] Caroline Chaux and Jean-Christophe pesquet 2005. Image Analysis Using a Dual-Tree M-Band Wavelet Transform. IEEE Transaction on image processing.

[27] [27] JunmeiZhong and RuolaNingoctober 2005. Image Denoising based on wavelets and Multifractals for singularity detection. IEEE transaction on image processing, vol.14, n0.10.

[28] [28]Mallat 1998. A wavelet tour of signal processing: San Diego, CA, USA : Academic Press.

[29] N.G Kinsbury1999. Image processing with complex wavelets. Phil.Trans. Royal Society London,.

[30] N.G Kinsbury 2000. A dual-tree complex wavelet transform with improved orthogonality and symmetry proprieties. In Proceedings of the EEE ,Int.Conf. on Image Proc.(ICIP).

[31] I.Selesnick,R.G.Baraniuk and N.G.Kingsbury2005.The dual-tree complex wavelet transform: IEE Signal Processing magazine, vol.22,n°6,pp.123-151.

[32] I.Selesnick and K.Li2003.video denoising using 2D and 3D dual-tree complex wavelet transforms.in wavelet applications in signal and and 3D dual-tree complex wavelet transforms. in wavelet applications in signal and image processing X(proc.SPIE 5207).

[33] L. Sendur and I. W. Selesnick2002. Bivariate shrinkage functions for wavelet-based de-noising exploiting interscale dependency. IEEE Trans. on Signal Processing. 50(11): 2744-2756, November.

[34] LaventSendur and Ivan Selesnick2002. Bivariate Shrinkage With Local Variance Estimation. IEEE SIGNAL PROCESSING LETTERS,DECEMBER, VOL.9,No.12.

[35] D L Donoho1995. De-noising by soft thresholding. IEE Trans. Info, Theory, 41(3),613-627,.